

Communication and Computation Assisted Sensing Information Freshness Performance Analysis in Vehicular Networks

Ning Jiang, Shi Yan, Zhuohan Liu, Chunjing Hu, Mugen Peng
State Key Laboratory of Networking and Switching Technology,
Beijing University of Posts and Telecommunications, Beijing, 100876, China.
Email: {creativejn,yanshi01,liuzhuohan,hucj,pmg}@bupt.edu.cn

Abstract—The timely sharing of raw sensing information in the vehicular networks (VNETs) is essential to safety. In order to improve the freshness of sensing information, joint scheduling of multi-dimensional resources such as communication and computation is required. However, the complex relevance among multi-dimensional resources is still unclear, and it is difficult to achieve efficient resource utilization. In this paper, we present a theoretical analysis for a novel metric Age of Information (AoI) on a communication and computation assisted spatial-temporal model. An uplink VNETs scenario where Road Side Units (RSUs) are deployed with computational resource is considered. The transmission and computation process is unified into a two-stage tandem queue and the expression of the average AoI is derived. The network interference is analyzed by modeling the VNETs as Cox Poisson Point Process based on stochastic geometry and the closed-form solution of the coverage probability and the expected data rate performance under the constraints of transmission resources is obtained. The simulation results reveal the basic relationship between communication and computation capacity and show that communication and computation should reach a tradeoff to improve resource utilization while ensuring real-time information requirement.

Index Terms—VNETs, transmission-computation tradeoff, Age of Information, tandem queue, spatial-temporal analysis

I. INTRODUCTION

The vehicular networks (VNETs) have been identified as one of the typical application scenarios of intelligent transportation system in the future which can support a variety of emerging services [1][2]. For time-sensitive applications, vehicles need to continuously share the environment status and road safety traffic to the road side unit (RSU) for analyzing the collected data to obtain real-time sensing information, thereby assisting the intelligent coordinated control. Age of Information (AoI) is a new key performance indicator (KPI) recently proposed for characterizing the freshness of the data [3]. In order to make adequate deployment, it is not only necessary to understand how the network affects the timeliness of information transmission, but also to extract the status information embedded in the data packet through computation processing.

Recently, AoI has been used in communication systems for various real-time applications (including VNETs) due to the high sensitivity to data freshness. The expression of peak and average AoI with preemption was deduced in [4], where the

influence of channel access control (such as ALOHA) was considered. In [5], the authors derived the peak AoI of large-scale IoT uplink networks under time-triggered and event-triggered traffic. In [6], the authors presented the AoI of computation intensive data in edge computing, and considered user local computing and remote computing on edge servers.

Although some scholars have carried out some research on AoI in wireless networks, the related research has the following limitations: Although there are many analysis models based on communication process, it may not be suitable to describe the actual traffic processing of data packets because the computation also impacts on the information freshness performance. Moreover, the freshness of information in large-scale wireless networks is usually leveraged based on queuing, while queuing analysis only captures time influence between transmitters and receivers [7]. Due to interference, the AoI is related with spatial distribution of active transmitter nodes, leading to the queue of the link to influence each other in space and time. In this paper, we investigate the communication and computation assisted spatial-temporal AoI performance in VNETs. The main contributions are as follows:

- A VNETs model is considered to establish spatial-temporal model using stochastic geometry and queuing theory to represent the macro and micro network performance: the intelligent vehicles transmit sensing data sampled by on-board sensors and implement data demodulation process in RSUs [8].
- A tandem queue model is proposed for the two stages of transmission and computation, and the analytical expression of the average AoI is derived. The Cox point process is used to represent the distribution of vehicles and RSUs [9]. Some closed-form solutions of KPIs such as uplink coverage probability and expected data rate are obtained.
- The simulation results evaluate the accuracy of the analysis and obtain the tradeoff between transmission and computation.

II. SYSTEM MODEL

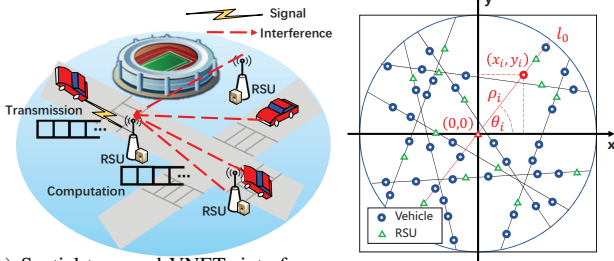
A. Vehicular Networks Spatial Model

As shown in Fig. 1(a), an uplink cellular-based VNETs model is considered. The intelligent vehicles can acquire

sensing information and transmit status update traffic to its associated RSU which is deployed with computational resource. We model the vehicles and RSUs by the Cox Poisson Point Process (PPP) which is illustrated in Fig. 1(b). The road is modeled as an independent motion-invariant Poisson line process ϕ_l with line intensity μ_l , which can be represented on a cylindrical space $\mathbf{C} := \mathbb{R} \times (0, \pi)$ generated by a homogeneous point process Ψ with intensity $\lambda_l = \mu_l/\pi$. Each node (ρ_j, θ_j) in Ψ is associated with the corresponding line L_j as follows

$$L_j(\rho_j, \theta_j) = \{(x, y) \in \mathbb{R}^2 \mid x \cos(\theta_j) + y \sin(\theta_j) = \rho_j\}, \quad (1)$$

where θ_j denotes the angle between the line L_j and the positive direction of the x -axis, and ρ_j denotes the distance between the line L_j and the origin [10]. By applying the Slivnyak theorem, the translation of the origin can be regarded as the process of adding a point to the space \mathbf{C} [11]. The tagged receive node is located at the origin. Therefore, we can set l_0 to be the line containing the tagged nodes, which represents the tagged line, and ϕ_{l_0} be the 1-D Poisson point process on this line. Φ is set to represent the Cox PPP which contains the all transmission nodes in VNETs.



(a) Spatial-temporal VNETs interference model. (b) Illustration of the Cox PPP of vehicles and RSUs.

Fig. 1. Spatial-temporal system model of the uplink VNETs based on queue and Cox PPP.

Next, the vehicles on each line are modeled as an independent one-dimensional (1-D) PPP with intensity λ_v and the RSUs are modeled with intensity λ_r by a similar process. Without loss of generality, we assume that the ratio of nodes in the transmitting state to all nodes is p and the transmission vehicles work on the same frequency band as the RSUs. The distribution of the nodes on the line is a PPP with intensity $\lambda_p = \lambda_{pv} + \lambda_{pr}$ [8]. The vehicle transmission power is P_v and only one antenna is configured.

The interference of the wireless channel can be expressed by a combination of standard path loss and small-scale fast fading, where the standard path loss can be expressed as $\|X_r\|^{-\alpha}$, where $\|X_r\|$ represents the distance between a tagged transmitter and its related receiver. Considering the high proportion of the Line of Sight (LOS) component between the tagged nodes in the case of accessing the nearest RSU, the small-scale fast fading can be assumed to be Rician fading. The probability density function (PDF) of Rician fading can be given by [12]

$$f_x(x) = (1 + K) e^{-K-(1+K)x} I_0 \left(2\sqrt{K(1+K)}x \right) \approx \sum_{i=1}^{N_K} w_i^K e^{-u_i^K x}, x \in [0, W], \quad (2)$$

where $I_0(\cdot)$ denotes zero-order modified Bessel function of the first kind, and K denotes the Rician factor which represents

the ratio of the power of the LOS component to the power of the diffuse component. N_K is the number of weighted terms which is related to the Rician factor. Besides, the formula must conform to the two constraints $\sum_{i=1}^{N_K} w_i^K = 1$ and $u_i^K > 0$.

To analyze the wireless link, the expression of signal-to-interference ratio of the transmission link is given by

$$SIR = \gamma_r = \frac{P_v h_r \|X_r\|^{-\alpha}}{I_{\phi_{l_0}} + I_{\Phi/\phi_{l_0}}}, \quad (3)$$

where h_r and $\|X_r\|^{-\alpha}$ respectively denote the Rician fading and path loss between the tagged transmitter and receiver. $g_l \sim \exp(1)$ denotes the exponential distribution of Rayleigh fading between the interference nodes and tagged receiver. $I_{\phi_{l_0}}$ denotes interference from nodes on the same road and $I_{\Phi/\phi_{l_0}}$ denotes the interference from nodes on different roads.

B. Transmission and Computation Assisted Temporal Model

A tagged link is formed as the transmitter-receiver pair. As depicted in Fig. 2, AoI is employed to measure the performance of the transmission and computation assisted system which is used to quantify the information freshness of the process from the generation of sensing information to the end of computation. When RSU does not demodulate the content of the data packet, the AoI on the tagged link increases linearly with a slope of 1. The AoI will reduce the time elapsed from the generation of the data packet to the completion of the computation. The process of data packages is subject to the First-Come-First-Served (FCFS) principle. The definition of AoI [3] is $\Delta(t) = t - A(t)$, where $\Delta(t)$ denotes the AoI of the link, and $A(t)$ denotes the end time of the tandem process. Average AoI is usually used as a performance metric to evaluate the freshness of information which can be obtained as $avgAoI = \lim_{T \rightarrow \infty} \frac{1}{T} \int_0^T \Delta(t) dt$ [3].

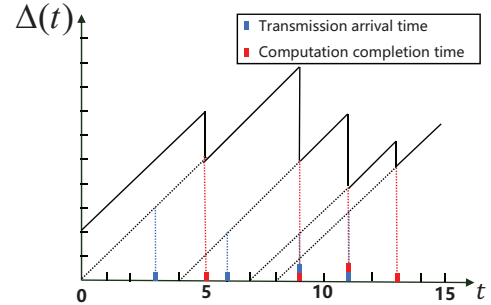


Fig. 2. Age of Information for transmission and computation tandem queue.

The two-stage tandem M/M/1 queue is used to establish the transmission and computation assisted model. $\mu_1 = \frac{bR}{L}$ is the transmission rate where b is the bandwidth, L is the packet size in bit and R is the expected data rate. The computation process is initiated after the transmission process ends. In the process unit of RSU, the CPU cycle frequency can be adjusted by voltage through dynamic voltage and frequency scaling (DVFS) technology, so the computation rate is $\mu_2 = f/L\kappa$ and the computation power is $P_c = \zeta f^3$ where κ denotes the number of CPU cycles required to process one bit and ζ is the

conversion factor depends on the average switched capacitance and the average activity [13].

III. PERFORMANCE ANALYSIS

In this section, we first obtain the transmission and computation assisted AoI analytical expressions represented by the M/M/1 tandem queue. Then we derive the closed-form solution of coverage probability and the expected data rate representing the uplink transmission performance of the VNETs.

A. Average Age of Information the Transmission-Computation tandem queue

As shown in Fig. 3, the information traffic from the source is transmitted in turn in the first queue, and then reaches the second queue to continue computation process. It is assumed that the traffic arriving at the first queue follows Poisson distribution, which means the sampling time interval of different data packets is the negative exponential distribution with the parameter λ .

The M/M/1 tandem queue conforms to the overtake-free and quasi-reversible properties [14]. An important feature of the quasi-reversible queue is that the Poisson traffic passing through the queue is statistically invariant and can produce a Poisson output traffic at the same rate, in other words, Poisson-in-Poisson-out. Therefore, the interaction between the transmission queue and the computation queue can be ignored when calculating the average AoI, and an approximate tractable result can be obtained.

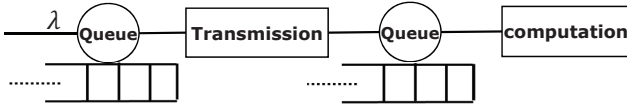


Fig. 3. The transmission-computation tandem queue for vehicle and tagged RSU.

Next, for a certain data packet in the system, the process is shown in Fig. 4. ω_n^1 denotes the queuing time of the first queue, τ_n^1 denotes the transmission time of the first queue, and $T_n^{(2)}$ is the time of the packet in the second queue.



Fig. 4. Packet process flow in sensing information traffic.

When calculating the average AoI, we only pay attention to the time interval distribution of each data packet sampling Y_n and the system time distribution T_n due to the fundamental formula $avgAoI = \left(E[T_n Y_n] + E\left[\frac{Y_n^2}{2}\right] \right) / E[Y_n]$ in [3].

Therefore, the sum of the service time in the first queue and the system time in the second queue can be approximated as the overall service time τ_n . Thus, $T_n = \omega_n^1 + \tau_n$, in which τ_n and T_n are independent. As shown in Fig. 5, ω_n^1 can be divided into two situations: if the current $n-1$ packets have been processed, ω_n^1 is 0, and if the current $n-1$ packets have

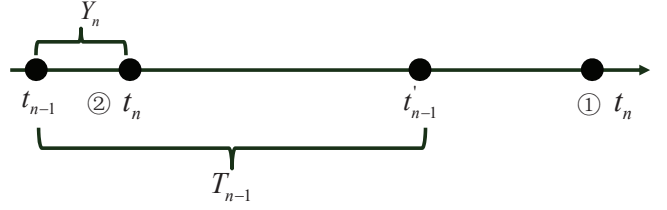


Fig. 5. Time period division between adjacent packets.

not been processed, $\omega_n^1 = T_{n-1} - Y_n$. Thus the expectation of ω_n^1 under condition $Y_n = y$ can be derived as

$$\begin{aligned} E[\omega_n^1 | Y_n = y] &= E[(T_{n-1} - Y_n)^+ | Y_n = y] \\ &= E[(T - Y)^+] = \int_y^\infty (t - y) f_T(t) dt. \end{aligned} \quad (4)$$

Then, the transmission rate and the computation rate are set to μ_1 and μ_2 , respectively. Based on the statistical independence of the queue, when $\mu_1 \neq \mu_2$, the distribution of the sojourn time of the tandem queue is given as

$$\begin{aligned} f_T(t) &= \int_0^t (\mu_1 - \lambda) e^{-(\mu_1 - \lambda)(t-y)} (\mu_2 - \lambda) e^{-(\mu_2 - \lambda)y} dy \\ &= \frac{(\mu_1 - \lambda)(\mu_2 - \lambda)}{\mu_1 - \mu_2} [e^{-(\mu_2 - \lambda)t} - e^{-(\mu_1 - \lambda)t}]. \end{aligned} \quad (5)$$

When $Y_n = y$, the conditional expectation of ω_n^1 is given as

$$\begin{aligned} E[\omega_n^1 | Y_n = y] &= \int_y^{+\infty} \eta (t - y) [e^{-(\mu_2 - \lambda)t} - e^{-(\mu_1 - \lambda)t}] dt \\ &= \eta \left[\frac{e^{-(\mu_2 - \lambda)y}}{(\mu_2 - \lambda)^2} - \frac{e^{-(\mu_1 - \lambda)y}}{(\mu_1 - \lambda)^2} \right], \end{aligned} \quad (6)$$

where $\eta = \frac{(\mu_1 - \lambda)(\mu_2 - \lambda)}{\mu_1 - \mu_2}$.

So the expectation of $\omega_n^1 Y_n$ is given as

$$\begin{aligned} E[\omega_n^1 Y_n] &= \int_0^\infty y \cdot E[\omega_n^1 | Y_n = y] \cdot f_Y(y) dy \\ &= \int_0^\infty y \cdot \eta \left[\frac{e^{-(\mu_2 - \lambda)y}}{(\mu_2 - \lambda)^2} - \frac{e^{-(\mu_1 - \lambda)y}}{(\mu_1 - \lambda)^2} \right] \cdot \lambda e^{-\lambda y} dy \\ &= \lambda \eta \left[\frac{1}{(\mu_2 - \lambda)^2 \mu_2^2} - \frac{1}{(\mu_1 - \lambda)^2 \mu_1^2} \right]. \end{aligned} \quad (7)$$

The total service time expectation is approximately the sum of the service time expectation of the two queues, and the average AoI of the tandem queue is derived as follows

$$\begin{aligned} avgAoI &= \frac{E[\omega_n^1 Y_n] + E[\tau_n Y_n] + E\left[\frac{Y_n^2}{2}\right]}{E[Y_n]} \\ &\approx \frac{\lambda \eta \left[\frac{1}{(\mu_2 - \lambda)^2 \mu_2^2} - \frac{1}{(\mu_1 - \lambda)^2 \mu_1^2} \right] + \frac{1}{\lambda} \cdot \left(\frac{1}{\mu_1} + \frac{1}{\mu_2} \right) + \frac{1}{\lambda^2}}{\frac{1}{\lambda}} \\ &= \lambda^2 \eta \left[\frac{1}{(\mu_2 - \lambda)^2 \mu_2^2} - \frac{1}{(\mu_1 - \lambda)^2 \mu_1^2} \right] + \frac{1}{\mu_1} + \frac{1}{\mu_2} + \frac{1}{\lambda}. \end{aligned} \quad (8)$$

The average AoI in the tandem queue is given as follows when $\mu_1 = \mu_2$

$$avgAoI \approx \frac{2\lambda^2}{\mu^3} + \frac{2\lambda^2}{(\mu - \lambda)\mu^2} + \frac{2}{\mu} + \frac{1}{\lambda}. \quad (9)$$

Proof. See Appendix A. \square

B. Transmission Data Rate

To facilitate the performance analysis of the proposed model, we first derive the uplink coverage probability $P(P_v, T)$ where P_v is the vehicle transmission power and T is the threshold. T can be regarded as an indicator that reflects quality-of-service (QoS). The larger value of T may represent higher requirement for SIR, which means that better received signal quality is required to correctly demodulate useful signals. The uplink coverage probability is given as

$$P(P_v, T) = \sum_{i=1}^{N_K} w_i^K \exp \left(-\varepsilon_1 \left(\lambda_{pr} \left(\frac{P_r}{P_v} \right)^{\frac{1}{\alpha}} + \lambda_{pv} \right) - \varepsilon_2 \left(\lambda_{pr} \left(\frac{P_r}{P_v} \right)^{\frac{2}{\alpha}} + \lambda_{pv} \right) \right), \quad (10)$$

where $\varepsilon_1 = \frac{2\pi(u_i^K T)^{\frac{1}{\alpha}} \|X_r\|}{\sin(\frac{\pi}{\alpha})\alpha}$ and $\varepsilon_2 = \frac{2\pi^3 \lambda_l (u_i^K T)^{\frac{2}{\alpha}} \|X_r\|^2}{\sin(\frac{2\pi}{\alpha})\alpha}$.

When T and P_v is fixed, the closed-form solution of the expected data rate can be obtained according to $R = \log_2(1 + T) P(P_v, T)$.

Proof. See Appendix B. \square

IV. NUMERICAL RESULTS

In this section, we present the simulation results of the following three parts: the average AoI of the transmission-computation tandem queue; the coverage probability and expected data rate of the uplink VNETs; the average AoI with different transmission and computation capability. Monte Carlo method is used to verify the correctness of theoretical analysis. The simulation range is a circular area with radius 1 km, the intensity of roads λ_l is $5 \times 10^{-3}/\pi$, the distance between the tagged nodes $\|X_r\|$ is 20 m. The intensity of transmission vehicle λ_{pv} and RSU λ_{pr} are 1×10^{-2} and 3×10^{-3} , respectively. The bandwidth b is 2 MHz. The data packet sampling rate λ is 100 /s with packet size L set to be 1×10^3 bits. Path loss exponent α is set to 3, and RSU transmission power P_r is 33 dBm. We assume that RSUs are deployed with sufficient computation resources which the CPU cycles required for computing one input bit κ is 1×10^3 cycles/bit [15]. The considered communication resource is the vehicle transmission power P_v in the range of [15, 30] dBm and the considered computation resource is CPU cycle frequency f which is $[0.15, 0.45] \times 10^9$ cycles/bit. The conversion factor ζ is 1.25×10^{-26} J/cycle. The Rician fading coefficients w_i^K and u_i^K [13] are listed in Table I.

TABLE I
RICIAN FADING SIMULATION PARAMETERS

Term Index	$n = 1$	$n = 2$	$n = 3$	$n = 4$
w_i^K	-0.8993	5.9324	-5.4477	1.4145
u_i^K	1.2475	1.4298	1.7436	2.0326

Fig. 6 shows the average AoI with different transmission rates and computation rates when the data packet sampling rate is fixed to 500 /s for obvious comparison. The approximation

is based on the statistical characteristics of the Poisson-in-Poisson-out of the tandem M/M/1 and the queue interaction is ignored. The analytical results are consistent with the results of the simulations which confirms the validity of the assumption and the accuracy of expressions. When the transmission and computation rate increase, the average AoI will decrease. Moreover, the corresponding law of the two rates to the average AoI is the same. In other words, increasing the same amount of transmission or computation rate will result the same reduction in average AoI. Further analysis shows that with the continuous increase of transmission rate and computation rate, the reduction degree of the average AoI becomes smaller and tends to be stable.

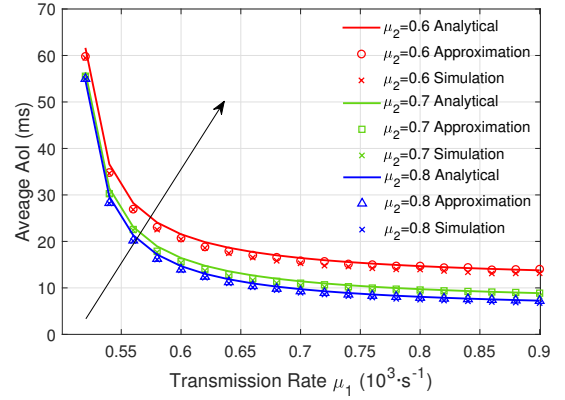
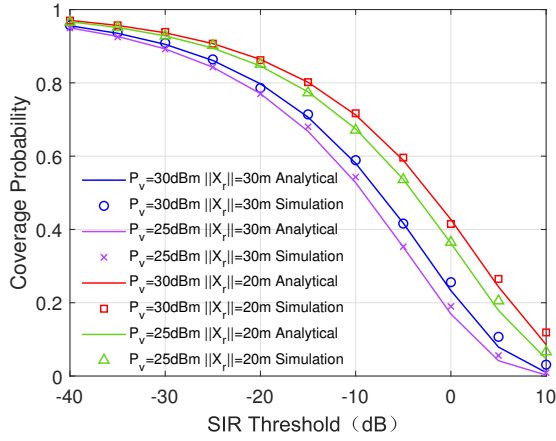


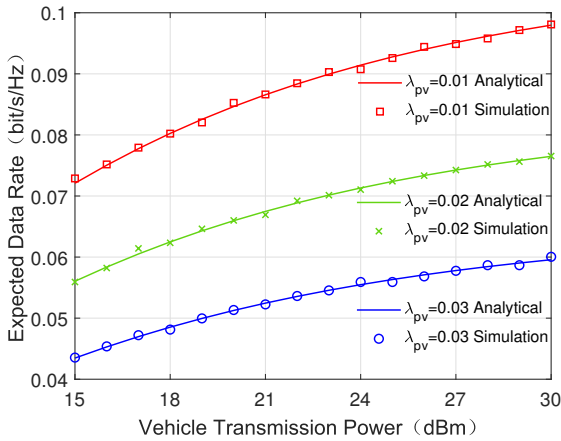
Fig. 6. Average AoI with different transmission rates versus computation rate.

Fig. 7 shows the uplink coverage probability and the expected data rate. As can be seen in Fig. 7(a), for any vehicle transmission power and the distance between the tagged transmitter-receiver, when the SIR threshold increases, the coverage probability decreases. For a larger distance between a vehicle and a tagged RSU, the signal power received by a tagged receive RSU will experience larger path loss, thereby reducing coverage performance; when the vehicle transmission power increases, the interference transmission power of the RSU remains unchanged in this case, while the useful signal power of the tagged receiving node will increase, thereby achieving better coverage performance. Fig. 7(b) shows the expected data rate under different vehicle transmission power and different distances between the tagged transmitter-receiver. The T is set to -10 dB. With the increase of vehicle transmission power, the expected data rate increases. When the intensity of transmit vehicles in the network is fixed, by increasing the transmission power of the transmit vehicles, the transmission rate will increase monotonically, contributing to reducing the average AoI and improving information freshness of data in the transmission process.

Fig. 8 shows the trend of the average AoI with different vehicle transmission power and computation power. Fig. 8(a) shows that by increasing the vehicle transmission power, the transmission rate of the data packet will increase. The same to computation power, increasing computation power also results in a better average AoI. As shown in Fig. 8(b), when the computation capability is fixed, blindly improving



(a) Coverage probability with different SIR threshold versus vehicle transmission power and $\|X_r\|$.



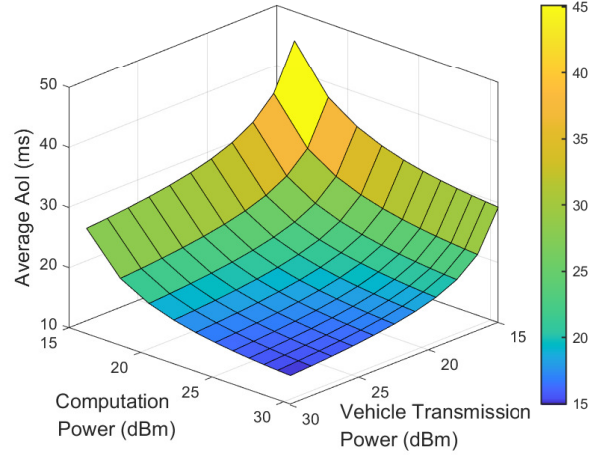
(b) Expected data rate with different vehicle transmission power versus intensity of transmit vehicle.

Fig. 7. Uplink coverage probability and expected data rate in VNETs.

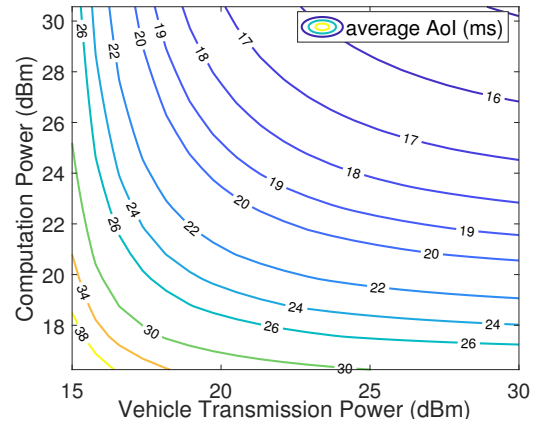
the communication capacity will not effect on the obvious improvement on AoI. When computation power is 20 dBm and average AoI is 22 ms, the transmission power is about 25 – 30 dBm. Increasing the transmission power can not significantly enhance average AoI, which is the same to computation. So if the transmission capacity does not match the computation capacity, it is not only difficult to guarantee the information freshness, but also a waste of resources, e.g. if the computation rate is too slow to execute tasks timely, increasing the transmission rate blindly is useless and leads to radio frequency (RF) power consumption waste and vice versa.

V. CONCLUSION

In this paper, the aim is to access the freshness of sensing information based on transmission-computation process in uplink VNETs scenario where vehicles are deployed for sensing data transmission and RSUs are served to enhance computation. A two-stage tandem queue is proposed to analyze the communication and computation assisted temporal performance of AoI and the Cox PPP is used to model spatial



(a) The trend of the average AoI versus vehicle transmission power and computation power in mesh.



(b) Communication and Computation tradeoff for average AoI.

Fig. 8. Communication and Computation Assisted Spatial-Temporal average AoI Performance

distribution of vehicles and RSUs. The closed-form solutions of the coverage probability and expected data rate as well as the analytical expressions of the average AoI of the tandem queue are derived. The simulation results verify the accuracy of these analysis and show that a tradeoff scheduling between communication and computation capacity will contribute to enhancing sensing information freshness and making efficient use of resources.

APPENDIX

A. Proof of average AoI when $\mu_1 = \mu_2$

The statistical independence characteristics are

$$f_T(t) = (\mu - \lambda)^2 t e^{-(\mu-\lambda)t}. \quad (11)$$

Then we can derive the conditional expectation of ω_n^1 when $Y_n = y$ and $\mu_1 = \mu_2$. The expectation of $\omega_n^1 Y_n$ can also be obtained by the same method as (7):

$$\begin{aligned} E[\omega_n^1 Y_n] &= \int_0^\infty y \cdot \left[y e^{-(\mu-\lambda)y} + \frac{2e^{-(\mu-\lambda)y}}{\mu-\lambda} \right] \cdot \lambda e^{-\lambda y} dy \\ &= \lambda \left[\frac{2}{\mu^3} + \frac{2}{(\mu-\lambda)\mu^2} \right]. \end{aligned} \quad (12)$$

so the average AoI when $\mu_1 = \mu_2$ is given as follows

$$\begin{aligned} \text{avgAoI} &= \frac{E[\omega_n^1 Y_n] + E[\tau_n Y_n] + E\left[\frac{Y_n^2}{2}\right]}{E[Y_n]} \\ &\approx \frac{\lambda \left[\frac{2}{\mu^3} + \frac{2}{(\mu-\lambda)\mu^2} \right] + \frac{1}{\lambda} \cdot \left(\frac{1}{\mu} + \frac{1}{\mu} \right) + \frac{1}{\lambda^2}}{\frac{1}{\lambda}} = \frac{2\lambda^2}{\mu^3} + \frac{2\lambda^2}{(\mu-\lambda)\mu^2} + \frac{2}{\mu} + \frac{1}{\lambda}, \end{aligned} \quad (13)$$

the proof is finished.

B. Proof of $P(P_v, T)$

In the uplink VNETs scenario, the coverage probability can be calculated as

$$\begin{aligned} P(P_v, T) &= P[\gamma_r \geq T] = P\left[h_r \geq \frac{T \|X_r\|^\alpha}{P_v} \left(I_{\phi_{l_0}} + I_{\Phi/\phi_{l_0}} \right)\right] \\ &\stackrel{(a)}{=} \sum_{i=1}^{N_K} w_i^K \mathcal{L}_{I_{\phi_{l_0}}}(\omega) \mathcal{L}_{I_{\Phi/\phi_{l_0}}}(\omega), \end{aligned} \quad (14)$$

where (a) follows that the interference can be approximated by (2) for Rician fading and set $\omega = \frac{u_i^K T \|X_r\|^\alpha}{P_v}$.

The Laplace transform of the interference of RSUs from the same road can be derived as

$$\begin{aligned} &E \left[\prod_{\|X_l^r\| \in \phi_{l_0}} e^{-\omega P_r g_l \|X_l^r\|^{-\alpha}} \right] \\ &\stackrel{(a)}{=} \exp \left(- \int_0^\infty E_{g_l} \left[1 - e^{-\omega P_r g_l \|X_l^r\|^{-\alpha}} \right] \lambda_{pr} \|X_l^r\| d \|X_l^r\| \right) \\ &\stackrel{(b)}{=} \exp \left(-2\lambda_{pr} (w P_r)^{\frac{1}{\alpha}} E \left[g_l^{\frac{1}{\alpha}} \right] \Gamma \left(1 - \frac{1}{\alpha} \right) \right), \end{aligned} \quad (15)$$

where (a) follows that expectation of the independent PPP can act on Rayleigh fading g_l , and (b) follows the properties of the Gamma function $E \left[g_l^{\frac{1}{\alpha}} \right] \Gamma \left(1 - \frac{1}{\alpha} \right) = \Gamma \left(1 + \frac{1}{\alpha} \right) \Gamma \left(1 - \frac{1}{\alpha} \right) = \frac{\pi}{\sin(\frac{\pi}{\alpha})\alpha}$. For the interference from vehicles, the close form solution can be obtained by a similar method. Then the interference of nodes on the same road can be derived by substituting (16) and the solution to $\mathcal{L}_{I_{\phi_{l_0}}}(\omega) =$

$$\begin{aligned} &E \left[\prod_{\|X_l^r\|, \|X_l^v\| \in \phi_{l_0}} e^{-\omega P_r g_l \|X_l^r\|^{-\alpha} - \omega P_v g_l \|X_l^v\|^{-\alpha}} \right] \\ \mathcal{L}_{I_{\phi_{l_0}}}(\omega) &= \exp \left(- \frac{2\pi (u_i^K T)^{\frac{1}{\alpha}} \|X_r\|}{\sin(\frac{\pi}{\alpha})\alpha} \left(\lambda_{pr} \left(\frac{P_r}{P_v} \right)^{\frac{1}{\alpha}} + \lambda_{pv} \right) \right). \end{aligned} \quad (16)$$

Next is the Laplace transform of the interference of RSUs from different roads

$$\begin{aligned} &E \left[\prod_{\|X_j^r\| \in \Phi/\phi_{l_0}} e^{-\omega P_r g_l \|X_j^r\|^{-\alpha}} \right] \\ &\stackrel{(a)}{=} \prod_{\rho_j \in \Psi} \exp \left(-2\lambda_{pr} \int_0^\infty \frac{w P_r (\sqrt{\rho_j^2 + t^2})^{-\alpha}}{1 + w P_r (\sqrt{\rho_j^2 + t^2})^{-\alpha}} dt \right) \\ &\stackrel{(b)}{=} \exp \left(2\pi \lambda_l \int_0^\infty 1 - e^{-2\lambda_{pr} \Delta(v)} dv \right) \\ &\stackrel{(c)}{\approx} \exp \left(2\pi \lambda_l \int_0^\infty 2\lambda_{pr} \Delta(v) dv \right) \\ &\stackrel{(d)}{=} \exp \left(-\pi^2 \lambda_l \lambda_{pr} (w P_r)^{\frac{2}{\alpha}} \frac{2\pi}{\sin(\frac{2\pi}{\alpha})\alpha} \right), \end{aligned} \quad (17)$$

where (a) follows the Euclidean distance from the transmitter to the tagged RSU and the probability generating function (PGFL) of the 1-D PPP $l(\rho_j, \theta_j)$, and (b) follows $\Delta(v) = \int_0^\infty \frac{w P_r (\sqrt{v^2 + t^2})^{-\alpha}}{1 + w P_r (\sqrt{v^2 + t^2})^{-\alpha}} dt$ and PGFL of independent line process Ψ [12], and (c) using Taylor expansion to obtain the

first two components with a large proportion for computation approximation: $e^x = \sum_{s=0}^{+\infty} \frac{x^s}{s!} = 1 + x + o(x)$. $2\lambda_{pr} \Delta(v)$ is small enough to be ignored when $s > 1$. Step (d) uses the transformation of the polar coordinate.

The close form solution can also be obtained for the interference from vehicles using the similar method as (18). Then the interference of nodes on different roads can be derived by substituting (18) and the solution to $\mathcal{L}_{I_{\Phi/\phi_{l_0}}}(\omega) =$

$$\begin{aligned} &E \left[\prod_{\|X_j^r\|, \|X_j^v\| \in \Phi/\phi_{l_0}} e^{-\omega P_r g_l \|X_j^r\|^{-\alpha} - \omega P_v g_l \|X_j^v\|^{-\alpha}} \right] \\ \mathcal{L}_{I_{\Phi/\phi_{l_0}}}(\omega) &= \exp \left(- \frac{2\pi^3 \lambda_l (u_i^K T)^{\frac{2}{\alpha}} \|X_r\|^2}{\sin(\frac{2\pi}{\alpha})\alpha} \left(\lambda_{pr} \left(\frac{P_r}{P_v} \right)^{\frac{2}{\alpha}} + \lambda_{pv} \right) \right). \end{aligned} \quad (18)$$

Substituting (17) and (19) into (15) yields the result.

REFERENCES

- [1] H. Zhou, W. Xu, J. Chen, and W. Wang, "Evolutionary v2x technologies toward the internet of vehicles: Challenges and opportunities," *Proceedings of the IEEE*, vol. 108, no. 2, pp. 308–323, 2020.
- [2] X. Zhang, M. Peng, S. Yan, and Y. Sun, "Deep-reinforcement-learning-based mode selection and resource allocation for cellular v2x communications," *IEEE Internet of Things Journal*, vol. 7, no. 7, pp. 6380–6391, 2019.
- [3] S. Kaul, R. Yates, and M. Gruteser, "Real-time status: How often should one update?" in *2012 Proceedings IEEE INFOCOM*. IEEE, 2012, pp. 2731–2735.
- [4] H. H. Yang, C. Xu, X. Wang, D. Feng, and T. Q. Quek, "Understanding age of information in large-scale wireless networks," *IEEE Transactions on Wireless Communications*, vol. 20, no. 5, pp. 3196–3210, 2021.
- [5] M. Emara, H. ElSawy, and G. Bauch, "Prioritized multistream traffic in uplink iot networks: Spatially interacting vacation queues," *IEEE Internet of Things Journal*, vol. 8, no. 3, pp. 1477–1491, 2020.
- [6] Q. Kuang, J. Gong, X. Chen, and X. Ma, "Age-of-information for computation-intensive messages in mobile edge computing," in *2019 11th International Conference on Wireless Communications and Signal Processing (WCSP)*. IEEE, 2019, pp. 1–6.
- [7] Y. Sun, E. Uysal-Biyikoglu, R. D. Yates, C. E. Koksall, and N. B. Shroff, "Update or wait: How to keep your data fresh," *IEEE Transactions on Information Theory*, vol. 63, no. 11, pp. 7492–7508, 2017.
- [8] S. Yan, X. Zhang, H. Xiang, and W. Wu, "Joint access mode selection and spectrum allocation for fog computing based vehicular networks," *IEEE Access*, vol. 7, pp. 17 725–17 735, 2019.
- [9] M. N. Sial, Y. Deng, J. Ahmed, A. Nallanathan, and M. Dohler, "Stochastic geometry modeling of cellular v2x communication over shared channels," *IEEE Transactions on Vehicular Technology*, vol. 68, no. 12, pp. 11 873–11 887, 2019.
- [10] C.-S. Choi and F. Baccelli, "An analytical framework for coverage in cellular networks leveraging vehicles," *IEEE Transactions on Communications*, vol. 66, no. 10, pp. 4950–4964, 2018.
- [11] M. Haenggi, *Stochastic geometry for wireless networks*. Cambridge University Press, 2012.
- [12] X. Yang and A. O. Fapojuwo, "Coverage probability analysis of heterogeneous cellular networks in rician/rayleigh fading environments," *IEEE Communications Letters*, vol. 19, no. 7, pp. 1197–1200, 2015.
- [13] J. M. Rabaey, A. P. Chandrakasan, and B. Nikolić, *Digital integrated circuits: a design perspective*. Pearson education Upper Saddle River, NJ, 2003, vol. 7.
- [14] I. Koukoutsidis, "Age of information in an overtake-free network of quasi-reversible queues," in *2020 28th International Symposium on Modeling, Analysis, and Simulation of Computer and Telecommunication Systems (MASCOTS)*. IEEE, 2020, pp. 1–6.
- [15] F. Wang, J. Xu, X. Wang, and S. Cui, "Joint offloading and computing optimization in wireless powered mobile-edge computing systems," *IEEE Transactions on Wireless Communications*, vol. 17, no. 3, pp. 1784–1797, 2017.